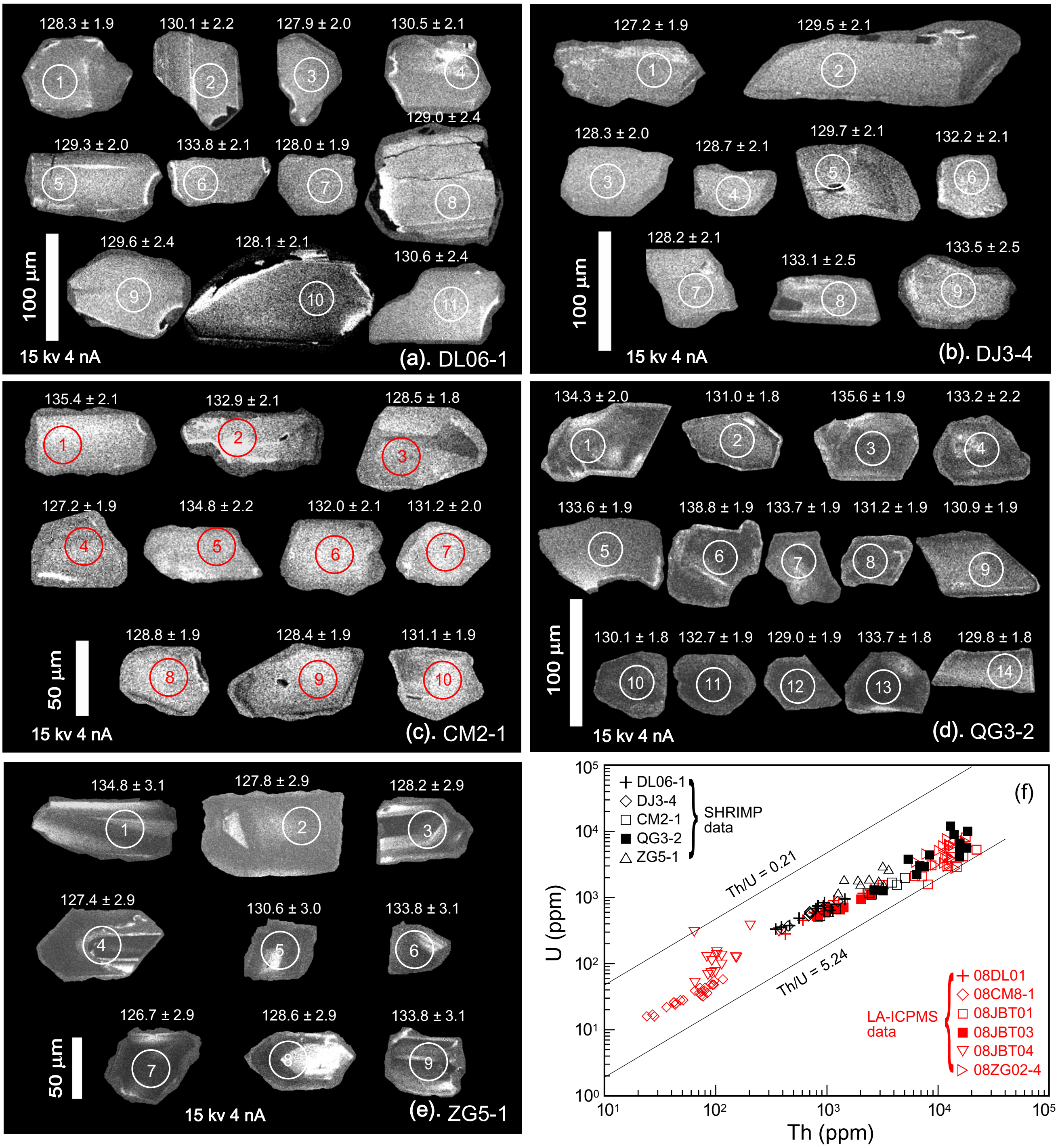

Fig. DR1 (Zhu et al.)

Cathodoluminescence (CL) images of zircon SHRIMP dating for rocks of the Comei large igneous province, southeastern Tibet. Circles indicate the locations of SHRIMP U-Pb dating, which were performed at the Beijing SHRIMP II Center, Chinese Academy of Geological Sciences. U vs. Th plot (f) showing all analyzed zircons are magmatic.

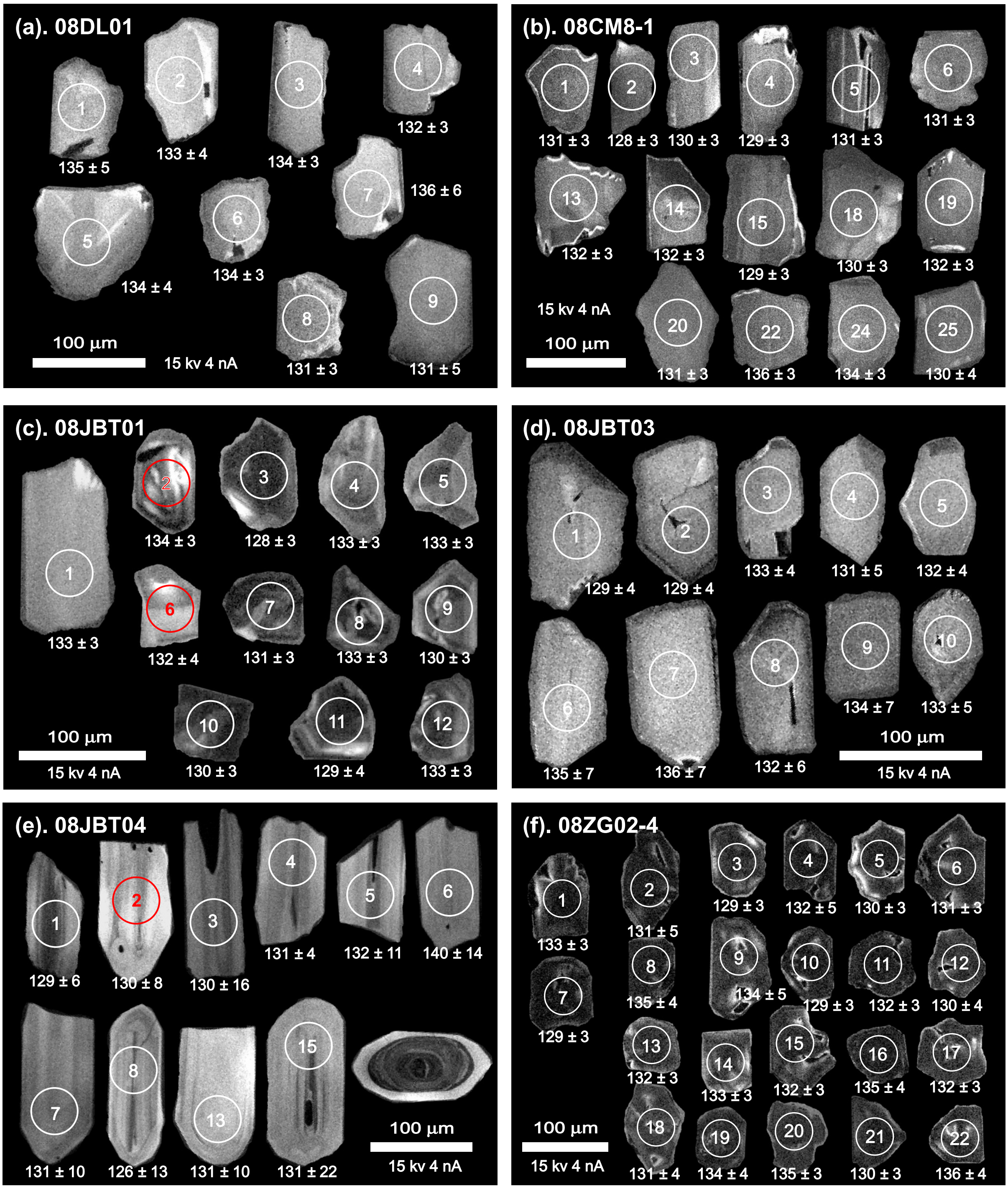

Fig. DR2 (Zhu et al.)

Cathodoluminescence (CL) images of zircon LA-ICPMS dating for rocks of the Comei large igneous province, southeastern Tibet. Circles indicate the locations of LA-ICPMS U-Pb dating, which were performed at the Institute of Geology and Geophysics, Chinese Academy of Sciences, China.

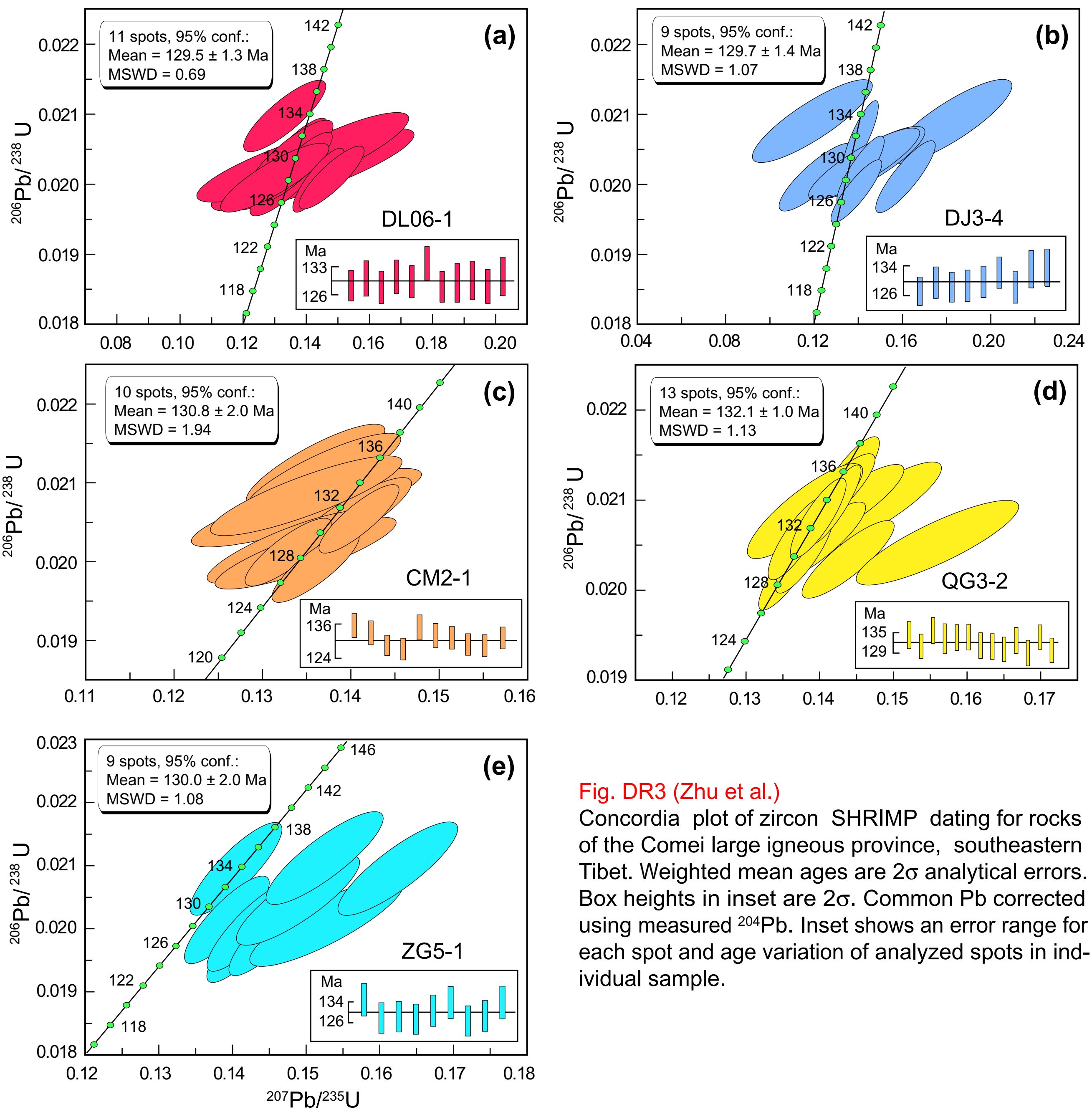

Fig. DR3 (Zhu et al.)

Concordia plot of zircon SHRIMP dating for rocks of the Comei large igneous province, southeastern Tibet. Weighted mean ages are 2σ analytical errors. Box heights in inset are 2σ. Common Pb corrected using measured ^{204}Pb. Inset shows an error range for each spot and age variation of analyzed spots in individual sample.

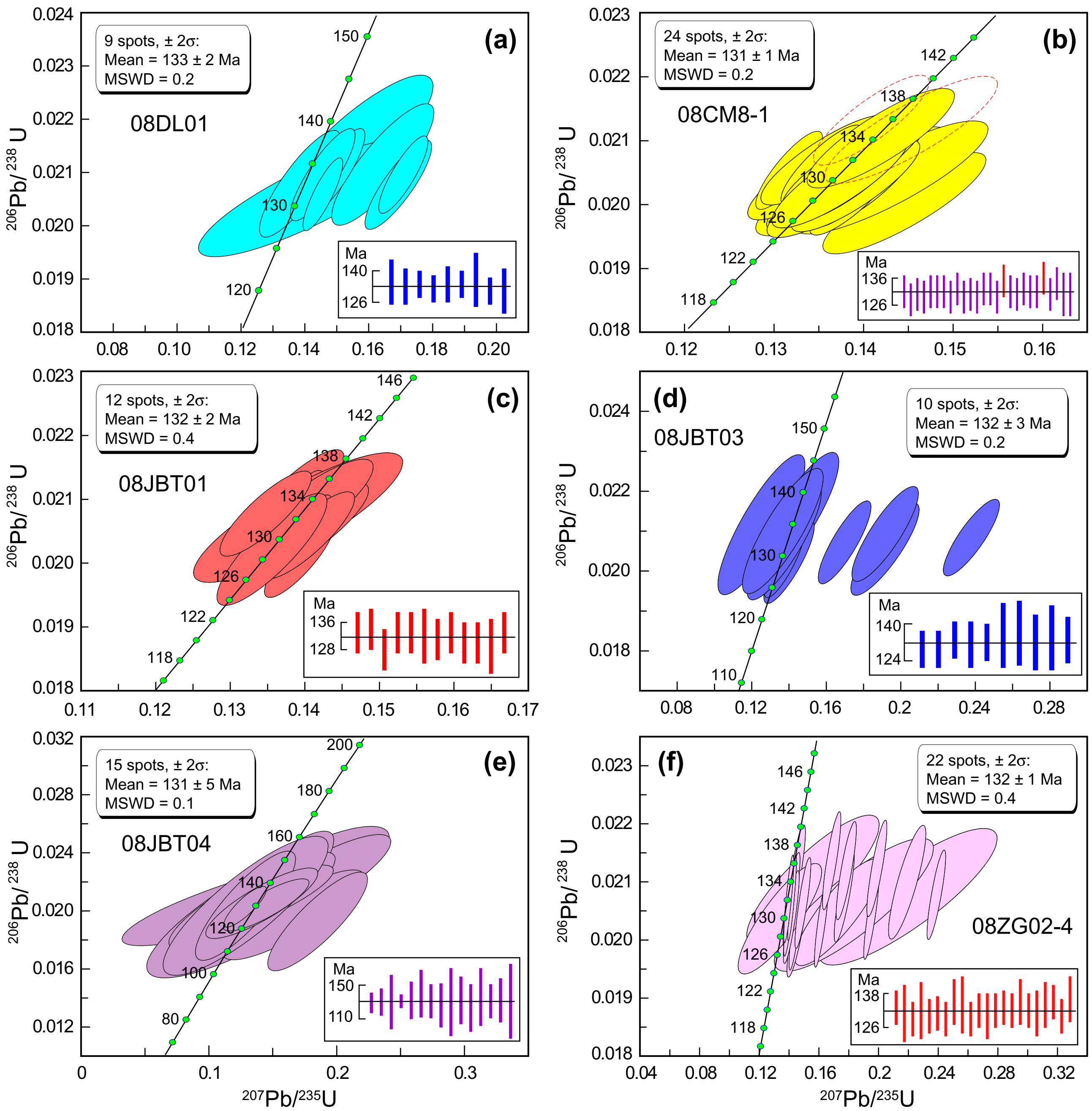

Fig. DR4 (Zhu et al.)

Concordia plot of zircon LA-ICPMS dating for rocks of the Comei large igneous province, southeastern Tibet. Weighted mean ages are 2σ analytical error. Common lead was corrected using the common lead correction function proposed by Anderson (2002). Box heights in inset are 2σ. Inset shows an error range for each spot and age variation of analyzed spots in individual sample.

TABLE DR1. SUMMARY OF ZIRCON U-PB ISOTOPIC AGES FOR SAMPLES OF THE COMEI LIP IN SOUTHEASTERN TIBET

No.	Sample	Location	GPS position	Rock unit	Rock type	Dating method	Age (Ma)*	Reference
1	YM04-1	Western Yamzho Yum Tso	N29.100°, E90.379°	Late Triassic strata	Diabasic dike	SHRIMP	134.1 ± 2.0	[1]
2	YM04-4	Western Yamzho Yum Tso	N28.939°, E90.385°	Late Triassic strata	Diabasic dike	SHRIMP	133.4 ± 1.6	[1]
3	SX(10)-1	Rimowa village	N28.748°, E90.747°	Sangxiu Formation	Dacite	SHRIMP	133.0 ± 3.0	[2]
4	08JBT04	Rimowa village	N28.746°, E90.715°	Sangxiu Formation	Dacite	LA-ICPMS	131 ± 5	[3]
5	DL06-1	Dalong village	N28.847°, E90.415°	Early to Middle Triassic strata	Diabasic dike	SHRIMP	129.5 ± 1.3	[3]
6	08DL01	Dalong village	N28.831°, E90.416°	Early to Middle Triassic strata	Diabasic dike	LA-ICPMS	133 ± 2	[3]
7	DJ3-4	North of Dongjia village	N28.674°, E90.833°	Early to Middle Jurassic strata	Gabbro	SHRIMP	129.7 ± 1.4	[3]
8	08JBT03	North of Dongjia village	N28.672°, E90.832°	Early to Middle Jurassic strata	Gabbro	LA-ICPMS	132 ± 3	[3]
9	08JBT01	North of Dongjia village	N28.633°, E90.818°	Early to Middle Jurassic strata	Diabasic dike	LA-ICPMS	132 ± 2	[3]
10	08CM8-1	North of Comei County	N28.489°, E91.430°	Middle Jurassic strata	Gabbro	LA-ICPMS	131 ± 1	[3]
11	CM2-1	North of Comei County	N28.512°, E91.462°	Middle Jurassic strata	Diabasic dike	SHRIMP	130.8 ± 2.0	[3]
12	ZG5-1	Southwestern Chigu Tso	N28.612°, E91.660°	Middle Jurassic strata	Pyroxenite	SHRIMP	130.0 ± 2.0	[3]
13	08ZG02-4	Southwestern Chigu Tso	N28.607°, E91.688°	Middle Jurassic strata	Gabbro	LA-ICPMS	132 ± 1	[3]
14	QG3-2	Qonggyai reservoir	N28.949°, E91.648°	Late Triassic strata	Diabasic dike	SHRIMP	132.2 ± 1.1	[3]
15	CN20-2	Kada village	N28.061°, E92.366°	Lakang Formation	Gabbro	SHRIMP	131.1 ± 6.1	[4]

**Note*: Ages are listed with 2σ uncertainty. [1] = re-calculated from Jiang et al. (2006); [2] = Zhu et al. (2005); [3] = this study; [4] = Zhu et al. (2008a).

References cited

Jiang, S.H., Nie, F.J., Hu, P., and Liu, Y., 2006, Important spreading event of the Neo-Tethys ocean during the Late Jurassic and Early Cretaceous: Evidence from Zircon U-Pb SHRIMP dating on diabase in Nagarze, southern Tibet: Acta Geologica Sinica, v. 80, p. 522–527.

Zhu, D.C., Pan, G.T., Mo, X.X., Wang, L.Q., Liao, Z.L., Jiang, X.S., and Geng, Q.R., 2005, SHRIMP U-Pb zircon dating for the dacite of the Sangxiu Formation in the central segment of Tethyan Himalaya and its implications: Chinese Science Bulletin, v. 50, p. 563–568.

Zhu, D.C., Mo, X.X., Pan, G.T., Zhao, Z.D., Dong, G.C., Shi, Y.R., Liao, Z.L., and Zhou, C.Y., 2008a, Petrogenesis of the earliest Early Cretaceous basalts and associated diabases from Cona area, eastern Tethyan Himalaya in south Tibet: interaction between the incubating Kerguelen plume and eastern Greater India lithosphere?: Lithos, v. 100, p. 147–173, doi: 10.1016/j.lithos.2007.06.024.

TABLE DR2. SHRIMP ZIRCON AGE DATA FOR SAMPLES OF THE COMEI LIP IN SOUTHEASTERN TIBET

Spot	*f*206[c] (%)	U (ppm)	Th (ppm)	Th/U	$^{206}Pb^*$ (ppm)	$^{207}Pb^*/^{235}U$ (± 1σ)	$^{206}Pb^*/^{238}U$ (± 1σ)	$^{206}Pb/^{238}U$ (Ma; ± 1σ)
DL06-1 weighted mean (11 spots, 2σ level, MSWD = 0.69)								**129.5 ± 1.3**
1.1	0.78	830	951	1.15	14.4	0.148 ± 0.007	0.0201 ± 0.0003	128.3 ± 1.9
2.1	1.21	375	462	1.23	6.66	0.135 ± 0.009	0.0204 ± 0.0003	130.1 ± 2.2
3.1	1.00	742	826	1.11	12.9	0.134 ± 0.008	0.0200 ± 0.0003	127.9 ± 2.0
4.1	0.63	746	927	1.24	13.2	0.136 ± 0.007	0.0205 ± 0.0003	130.5 ± 2.1
5.1	0.90	678	798	1.18	11.9	0.137 ± 0.007	0.0203 ± 0.0003	129.3 ± 2.0
6.1	1.06	745	837	1.12	13.6	0.133 ± 0.009	0.0210 ± 0.0003	133.8 ± 2.1
7.1	0.34	943	1452	1.54	16.3	0.144 ± 0.005	0.0201 ± 0.0003	128.0 ± 1.9
8.1	2.51	483	562	1.16	8.6	0.142 ± 0.021	0.0202 ± 0.0004	129.0 ± 2.4
9.1	2.30	356	390	1.10	6.36	0.136 ± 0.020	0.0203 ± 0.0004	129.6 ± 2.4
10.1	1.59	636	1069	1.68	11.1	0.130 ± 0.011	0.0201 ± 0.0003	128.1 ± 2.1
11.1	1.54	332	347	1.05	5.92	0.148 ± 0.016	0.0205 ± 0.0004	130.6 ± 2.4
DJ3-4 weighted mean (9 spots, 2σ level, MSWD = 1.07):								**129.7 ± 1.4**
1.1	0.92	862	1253	1.45	14.9	0.139 ± 0.007	0.0199 ± 0.0003	127.2 ± 1.9
2.1	1.15	711	1025	1.44	12.5	0.144 ± 0.016	0.0203 ± 0.0003	129.5 ± 2.1
3.1	1.44	605	700	1.16	10.6	0.121 ± 0.011	0.0201 ± 0.0003	128.3 ± 2.0
4.1	0.48	652	893	1.37	11.3	0.141 ± 0.007	0.0202 ± 0.0003	128.7 ± 2.1
5.1	1.59	577	697	1.21	10.2	0.144 ± 0.017	0.0203 ± 0.0003	129.7 ± 2.1
6.1	0.50	574	716	1.25	10.3	0.141 ± 0.005	0.0207 ± 0.0003	132.2 ± 2.1
7.1	0.53	527	687	1.30	9.14	0.161 ± 0.009	0.0201 ± 0.0003	128.2 ± 2.1
8.1	2.06	369	448	1.21	6.75	0.119 ± 0.018	0.0209 ± 0.0004	133.1 ± 2.5
9.1	2.44	331	393	1.19	6.1	0.182 ± 0.018	0.0209 ± 0.0004	133.5 ± 2.5
CM2-1 weighted mean (10 spots, 2σ level, MSWD = 1.94)								**130.8 ± 2.0**
1.1	0.44	525	870	1.66	9.62	0.136 ± 0.005	0.0212 ± 0.0003	135.4 ± 2.1
2.1	0.70	665	1207	1.82	12.0	0.135 ± 0.007	0.0208 ± 0.0003	132.9 ± 2.1
3.1	0.21	1665	3856	2.32	28.8	0.133 ± 0.003	0.0201 ± 0.0003	128.5 ± 1.8
4.1	0.22	1542	4267	2.77	26.5	0.136 ± 0.003	0.0199 ± 0.0003	127.2 ± 1.9
5.1	0.50	600	1051	1.75	10.9	0.137 ± 0.006	0.0211 ± 0.0003	134.8 ± 2.2
6.1	0.80	594	1025	1.73	10.6	0.135 ± 0.009	0.0207 ± 0.0003	132.0 ± 2.1
7.1	0.38	1096	2543	2.32	19.4	0.140 ± 0.004	0.0206 ± 0.0003	131.2 ± 2.0
8.1	0.62	1395	2943	2.11	24.3	0.133 ± 0.006	0.0202 ± 0.0003	128.8 ± 1.9
9.1	0.97	1164	2418	2.08	20.3	0.135 ± 0.007	0.0201 ± 0.0003	128.4 ± 1.9
10.1	0.18	1960	5040	2.57	34.7	0.141 ± 0.003	0.0205 ± 0.0003	131.1 ± 1.9

QG3-2 weighted mean (13 spots, without spot 6.1, 2σ level, MSWD = 1.13)								**132.1 ± 1.0**
1.1	0.44	3745	5402	1.44	68	0.142 ± 0.004	0.0211 ± 0.0003	134.3 ± 2.0
2.1	0.51	2876	7505	2.61	51	0.140 ± 0.004	0.0205 ± 0.0003	131.0 ± 1.8
3.1	0.19	6560	15761	2.40	120	0.144 ± 0.003	0.0213 ± 0.0003	135.6 ± 1.9
4.1	0.51	4057	15577	3.84	73.2	0.138 ± 0.005	0.0209 ± 0.0004	133.2 ± 2.2
5.1	0.44	1286	2657	2.07	23.2	0.148 ± 0.006	0.0209 ± 0.0003	133.6 ± 1.9
6.1	0.09	9890	18474	1.87	185	0.145 ± 0.002	0.0218 ± 0.0003	138.8 ± 1.9
7.1	0.42	2984	6864	2.30	53.9	0.144 ± 0.005	0.0210 ± 0.0003	133.7 ± 1.9
8.1	0.12	4781	15629	3.27	84.5	0.137 ± 0.003	0.0206 ± 0.0003	131.2 ± 1.9
9.1	1.08	1254	3213	2.56	22.3	0.156 ± 0.007	0.0205 ± 0.0003	130.9 ± 1.9
10.1	0.18	4351	8355	1.92	76.3	0.138 ± 0.003	0.0204 ± 0.0003	130.1 ± 1.8
11.1	0.09	8857	13966	1.58	158	0.140 ± 0.003	0.0208 ± 0.0003	132.7 ± 1.9
12.1	0.28	5545	18091	3.26	96.6	0.136 ± 0.003	0.0202 ± 0.0003	129.0 ± 1.9
13.1	0.14	11853	12937	1.09	214	0.142 ± 0.003	0.0210 ± 0.0003	133.7 ± 1.8
14.1	0.57	2190	6428	2.94	38.5	0.144 ± 0.004	0.0203 ± 0.0003	129.8 ± 1.8
ZG5-1 weighted mean (9 spots, 2σ level, MSWD = 1.08)								**130.0 ± 2.0**
1.1	0.15	1171	1263	1.08	21.3	0.152 ± 0.005	0.0211 ± 0.0005	134.8 ± 3.1
2.1	0.08	1857	1429	0.77	32	0.142 ± 0.004	0.0200 ± 0.0005	127.8 ± 2.9
3.1	0.11	1761	2930	1.66	30.5	0.153 ± 0.007	0.0201 ± 0.0005	128.3 ± 2.9
4.1	0.12	2650	3598	1.36	45.5	0.145 ± 0.004	0.0200 ± 0.0005	127.4 ± 2.9
5.1	0.15	1581	2009	1.27	28	0.149 ± 0.006	0.0205 ± 0.0005	130.6 ± 3.0
6.1	0.17	1830	1904	1.04	33.1	0.140 ± 0.004	0.0210 ± 0.0005	133.8 ± 3.1
7.1	0.01	2966	3189	1.08	50.6	0.142 ± 0.004	0.0198 ± 0.0005	126.7 ± 2.9
8.1	0.12	1884	2394	1.27	32.7	0.139 ± 0.004	0.0202 ± 0.0005	128.6 ± 2.9
9.1	0.13	1545	3247	2.10	27.8	0.162 ± 0.005	0.0210 ± 0.0005	133.8 ± 3.1

Note: $f206^{c}$ denotes the proportion of common ^{206}Pb in total measured $^{206}Pb^{*}$. * denotes radiogenic lead.

Note 1: SHRIMP zircon U–Pb dating

Zircons were separated from samples using standard density and magnetic separation techniques at the Special Laboratory of the Geological Team of Hebei Province, China. Zircon grains, together with the zircon U-Pb standard TEMORA (Black et al., 2003), were cast in an epoxy mount, which was then polished to section the crystals in half for analysis. Zircons were documented with transmitted and reflected light micrographs as well as cathodoluminescence (CL) images to reveal their internal structures, and the mount was vacuum-coated with a 500-nm layer of high-purity gold. Under the guidance of zircon CL images, the zircons were analyzed for U-Pb isotopes and U, Th, and Pb concentrations using a SHRIMP II ion microprobe at the Beijing SHRIMP Center, Chinese Academy of Geological Sciences, Beijing, following the procedures reported by Liu et al. (2006). The U-Th-Pb isotopic ratios were determined relative to the TEMORA standard zircon corresponding to 417 Ma $^{206}Pb/^{238}U$ = 0.0668 (Black et al. 2003), and the absolute abundances of U-Th-Pb element were calibrated to the standard zircon SL13. Analyses of the TEMORA standard zircon were interspersed with unknown sample grains, following operating and data processing procedures described by Williams (1998). The reference zircon was analyzed after every fourth analysis. Measured compositions were corrected for common Pb using the ^{204}Pb method (Compston et al., 1984), and data processing was carried out using Isoplot (Ludwig, 2001). Uncertainties on individual analyses are reported at the 1-sigma level; mean ages for pooled $^{206}Pb/^{238}U$ results are quoted at the 2-sigma level.

References cited:

Black, L.P., Kamo, S.L., Allen, C.M., Aleinikoff, J.N., Davis, D.W., Korsch, R.J., and Foudoulis, C., 2003, TEMORA 1: A new zircon standard for Phanerozoic U-Pb geochronology: Chemical Geology, v. 200, p. 155-170.

Compston, W., Williams, I.S., Meyer, C., 1984, U-Pb geochronology of zircons from Lunar Breccia 73217 using a sensitive high mass resolution ion microprobe: Journal of Geophysical Research, v. 89, p. 525-534.

Liu, D.Y., Jian, P., Kröner, A., and Xu, S.T, 2006, Dating of prograde metamorphic events deciphered from episodic zircon growth in rocks of the Dabie–Sulu UHP complex, China: Earth and Planetary Science Letters, v. 250, p. 650-666.

Ludwig, K.R., 2001, Using Isoplot/Ex, Version 2.49: a geochronological toolkit for Microsoft Excel. Berkeley Geochronology Center Special Publication, No. 1a: 47.

Williams, I.S., 1998, U-Th-Pb geochronology by ion microprobe. In: McKibben, M.A., Shanks, W.C., Ridley, W.I., eds. Applications of Microanalytical Techniques to Understanding Mineralizing Processes: Reviews in Economic Geology, v. 7, p. 1-35.

TABLE DR3. ZIRCON LA-ICPMS U-PB DATA FOR SAMPLES OF THE COMEI LIP IN SOUTHEASTERN TIBET

Analysis	Th	U	Pb*	Th/U	$^{207}Pb^*/^{206}Pb^*$		$^{207}Pb^*/^{235}U$		$^{206}Pb^*/^{238}U$		$^{207}Pb^*/^{206}Pb$		$^{207}Pb^*/^{235}U$		$^{206}Pb^*/^{238}U$	
					Ratio	± 1σ	Ratio	± 1σ	Ratio	± 1σ	Age	± 1σ	Age	± 1σ	Age	± 1σ
08DL01: diabasic dike, 9 spots, 2σ level, mean = 133 ± 2 Ma, MSWD = 0.2																
1.1	1072	623	18.9	1.72	0.05633	0.00397	0.16400	0.01045	0.02114	0.00075	465	80	154	9	135	5
2.1	608	449	12.3	1.35	0.04837	0.00313	0.13842	0.00821	0.02078	0.00066	117	78	132	7	133	4
3.1	1155	889	25.1	1.30	0.05160	0.00239	0.14906	0.00629	0.02098	0.00055	268	51	141	6	134	3
4.1	918	679	19.5	1.35	0.05905	0.00265	0.16886	0.00683	0.02076	0.00055	569	45	158	6	132	3
5.1	770	579	16.4	1.33	0.05038	0.00250	0.14541	0.00662	0.02095	0.00057	213	57	138	6	134	4
6.1	2497	1283	39.9	1.95	0.05904	0.00194	0.17039	0.00506	0.02095	0.00048	569	30	160	4	134	3
7.1	423	279	8.8	1.52	0.08351	0.00646	0.15443	0.01654	0.02140	0.00093	1281	142	146	15	136	6
8.1	2126	1143	34.5	1.86	0.05131	0.00157	0.14550	0.00407	0.02058	0.00045	255	30	138	4	131	3
9.1	989	645	19.6	1.53	0.04976	0.00807	0.14080	0.02226	0.02052	0.00073	184	270	134	20	131	5
08CM8-1: gabbro, 24 spots (without spot 16.1, 22.1), 2σ level, mean = 131 ± 1 Ma, MSWD = 0.2																
1.1	94	48	1.92	1.94	0.04775	0.00109	0.13475	0.00284	0.02046	0.00040	87	22	128	3	131	3
2.1	84	36	1.83	2.30	0.05239	0.00237	0.14459	0.00599	0.02001	0.00052	302	50	137	5	128	3
3.1	74	33	1.45	2.20	0.05015	0.00139	0.14046	0.00358	0.02031	0.00042	202	27	133	3	130	3
4.1	24	16	0.64	1.51	0.04868	0.00168	0.13595	0.00440	0.02025	0.00044	132	38	129	4	129	3
5.1	28	16	0.74	1.76	0.04785	0.00198	0.13508	0.00522	0.02048	0.00048	92	49	129	5	131	3
6.1	43	24	1.00	1.77	0.04931	0.00132	0.13964	0.00347	0.02054	0.00042	163	26	133	3	131	3
7.1	97	55	2.15	1.75	0.04658	0.00093	0.13179	0.00244	0.02052	0.00040	28	21	126	2	131	3
8.1	72	43	1.68	1.70	0.05005	0.00125	0.13892	0.00319	0.02014	0.00041	197	24	132	3	129	3
9.1	42	26	1.09	1.65	0.04951	0.00150	0.14064	0.00395	0.02061	0.00044	172	31	134	4	132	3
10.1	48	28	1.27	1.75	0.04935	0.00209	0.13749	0.00540	0.02022	0.00049	164	49	131	5	129	3
11.1	90	49	2.02	1.83	0.04845	0.00102	0.13648	0.00266	0.02044	0.00040	121	21	130	2	130	3
12.1	71	36	1.52	1.98	0.04979	0.00122	0.13899	0.00315	0.02026	0.00041	185	24	132	3	129	3

13.1	44	25	1.16	1.73	0.04768	0.00178	0.13587	0.00477	0.02068	0.00046	83	44	129	4	132	3
14.1	77	32	1.53	2.40	0.04868	0.00144	0.13890	0.00380	0.02071	0.00044	132	30	132	3	132	3
15.1	80	43	1.99	1.86	0.04982	0.00183	0.13916	0.00471	0.02028	0.00047	187	39	132	4	129	3
16.1	45	25	1.26	1.80	0.04987	0.00237	0.14534	0.00636	0.02115	0.00055	189	55	138	6	135	3
17.1	75	38	1.69	1.97	0.04773	0.00114	0.13540	0.00301	0.02060	0.00041	86	24	129	3	131	3
18.1	51	28	1.27	1.83	0.04925	0.00159	0.13838	0.00417	0.02040	0.00044	160	34	132	4	130	3
19.1	42	26	1.14	1.62	0.04932	0.00153	0.14008	0.00404	0.02062	0.00044	163	32	133	4	132	3
20.1	27	17	0.82	1.57	0.04892	0.00196	0.13883	0.00518	0.02060	0.00048	144	46	132	5	131	3
21.1	96	48	2.29	2.00	0.04898	0.00153	0.13888	0.00402	0.02059	0.00045	147	32	132	4	131	3
22.1	67	34	1.65	1.97	0.04804	0.00155	0.14092	0.00425	0.02130	0.00046	101	35	134	4	136	3
23.1	116	58	2.83	2.00	0.04902	0.00194	0.13750	0.00502	0.02037	0.00049	149	44	131	4	130	3
24.1	65	39	1.88	1.69	0.04905	0.00202	0.14196	0.00542	0.02102	0.00051	150	47	135	5	134	3
25.1	36	22	1.17	1.62	0.04952	0.00272	0.13877	0.00708	0.02035	0.00056	173	69	132	6	130	4
26.1	79	39	2.17	2.01	0.05090	0.00276	0.14310	0.00713	0.02041	0.00058	236	64	136	6	130	4
08JBT01: diabasic dike, 12 spots, 2σ level, mean = 132 ± 2 Ma, MSWD = 0.4																
1.1	1388	834	25	1.66	0.04853	0.00188	0.13901	0.00494	0.02080	0.00049	125	42	132	4	133	3
2.1	8750	3025	114	2.89	0.04786	0.00160	0.13884	0.00426	0.02106	0.00047	92	35	132	4	134	3
3.1	17746	8002	254	2.22	0.05043	0.00121	0.13935	0.00305	0.02006	0.00040	215	23	132	3	128	3
4.1	16940	4135	181	4.10	0.04828	0.00099	0.13859	0.00261	0.02084	0.00040	113	21	132	2	133	3
5.1	12999	4082	156	3.18	0.04899	0.00102	0.14012	0.00267	0.02077	0.00040	147	21	133	2	133	3
6.1	6236	2099	81	2.97	0.06028	0.00360	0.13918	0.00923	0.02071	0.00067	614	88	132	8	132	4
7.1	12124	2951	129	4.11	0.05604	0.00225	0.13989	0.00576	0.02048	0.00051	454	49	133	5	131	3
8.1	8101	1565	76	5.18	0.04898	0.00222	0.14037	0.00585	0.02082	0.00053	147	52	133	5	133	3
9.1	22230	5240	220	4.24	0.04947	0.00113	0.13924	0.00293	0.02044	0.00041	170	22	132	3	130	3
10.1	14739	2857	137	5.16	0.04997	0.00159	0.14054	0.00410	0.02043	0.00045	194	32	134	4	130	3
11.1	3170	1532	51	2.07	0.04869	0.00670	0.13567	0.00485	0.02021	0.00058	133	38	129	4	129	4
12.1	7211	2058	80	3.50	0.06046	0.00155	0.13486	0.00404	0.02077	0.00044	620	32	128	4	133	3

08JBT03: gabbro, 10 spots, 2σ level, mean = 132 ± 3 Ma, MSWD = 0.2																
1.1	963	589	20.6	1.64	0.05054	0.00349	0.14076	0.00892	0.02021	0.00068	220	86	134	8	129	4
2.1	1413	703	22.7	2.01	0.04962	0.00278	0.13814	0.00712	0.02020	0.00058	177	68	131	6	129	4
3.1	2031	930	33.9	2.18	0.08317	0.00399	0.23875	0.00998	0.02082	0.00063	1273	39	217	8	133	4
4.1	1278	701	23.8	1.82	0.06790	0.00478	0.19219	0.01207	0.02053	0.00076	866	71	178	10	131	5
5.1	2488	1073	37.6	2.32	0.05975	0.00366	0.17054	0.00940	0.02070	0.00068	595	65	160	8	132	4
6.1	806	522	16.7	1.54	0.04317	0.00571	0.12581	0.01541	0.02114	0.00115	-114	156	120	14	135	7
7.1	1102	684	20.1	1.61	0.04912	0.00568	0.14428	0.01532	0.02131	0.00108	154	147	137	14	136	7
8.1	1177	656	19.4	1.79	0.04833	0.00503	0.13798	0.01322	0.02071	0.00095	115	131	131	12	132	6
9.1	835	502	18.7	1.66	0.04747	0.00538	0.13728	0.01431	0.02098	0.00103	73	142	131	13	134	7
10.1	1318	651	21.5	2.02	0.06674	0.00458	0.19230	0.01179	0.02091	0.00078	830	69	179	10	133	5
08JBT04: dacite, 15 spots, 2σ level, mean = 131 ± 5 Ma, MSWD = 0.1																
1.1	64	299	6.89	0.21	0.04605	0.00447	0.12876	0.01103	0.02028	0.00093		105	123	10	129	6
2.1	83	126	3.03	0.66	0.05163	0.00832	0.14532	0.02206	0.02042	0.00119	269	235	138	20	130	8
3.1	151	124	4.21	1.22	0.04605	0.01077	0.12917	0.02572	0.02035	0.00250		213	123	23	130	16
4.1	204	373	8.76	0.55	0.05177	0.00381	0.14626	0.00999	0.02050	0.00068	275	96	139	9	131	4
5.1	91	72	1.97	1.26	0.04917	0.01389	0.13988	0.03805	0.02064	0.00167	156	364	133	34	132	11
6.1	99	74	2.16	1.34	0.06016	0.01444	0.18189	0.04005	0.02193	0.00221	609	309	170	34	140	14
7.1	92	109	2.66	0.85	0.04898	0.01159	0.13841	0.03101	0.02050	0.00165	147	301	132	28	131	10
8.1	370	301	7.59	1.23	0.06122	0.01465	0.16642	0.03617	0.01972	0.00206	647	296	156	31	126	13
9.1	85	67	2.29	1.27	0.04605	0.04406	0.12918	0.04237	0.02035	0.00318		340	123	38	130	20
10.1	113	131	3.31	0.86	0.04711	0.01575	0.13438	0.04272	0.02070	0.00224	55	382	128	38	132	14
11.1	65	51	2.01	1.29	0.06978	0.04055	0.18537	0.02578	0.01927	0.00226	922	129	173	22	123	14
12.1	154	122	3.79	1.25	0.13342	0.02914	0.14806	0.03286	0.02138	0.00274	2143	220	140	29	136	17
13.1	102	148	3.46	0.69	0.05018	0.01083	0.14194	0.02877	0.02052	0.00161	203	285	135	26	131	10
14.1	113	96	3.29	1.18	0.04605	0.02319	0.13151	0.06491	0.02071	0.00207		668	125	58	132	13
15.1	102	134	3.06	0.76	0.05169	0.02350	0.14675	0.06237	0.02060	0.00346	272	508	139	55	131	22

08ZG02-4: gabbro, 22 spots, 2σ level, mean = 132 ± 1 Ma, MSWD = 0.4																
1.1	13426	3682	157	3.65	0.08326	0.00158	0.23836	0.00405	0.02077	0.00051	1275	24	217	3	133	3
2.1	13072	3901	178	3.35	0.06463	0.01251	0.18358	0.03490	0.02060	0.00076	762	431	171	30	131	5
3.1	14342	2736	139	5.24	0.05797	0.00123	0.16203	0.00314	0.02028	0.00050	529	25	152	3	129	3
4.1	11402	3287	149	3.47	0.07677	0.01392	0.21956	0.03892	0.02074	0.00078	1115	395	202	32	132	5
5.1	13693	6001	201	2.28	0.06940	0.00130	0.19514	0.00331	0.02040	0.00049	911	24	181	3	130	3
6.1	11626	3865	145	3.01	0.04991	0.00098	0.14086	0.00254	0.02047	0.00050	191	27	134	2	131	3
7.1	10179	5090	156	2.00	0.05246	0.00177	0.14588	0.00449	0.02017	0.00054	306	31	138	4	129	3
8.1	12826	6072	191	2.11	0.04983	0.00159	0.14512	0.00424	0.02113	0.00056	187	30	138	4	135	4
9.1	9406	3079	131	3.05	0.05396	0.01017	0.15642	0.02897	0.02103	0.00074	369	386	148	25	134	5
10.1	12088	7619	220	1.59	0.05201	0.00113	0.14503	0.00291	0.02023	0.00050	286	26	138	3	129	3
11.1	11149	5961	184	1.87	0.04996	0.00071	0.14269	0.00189	0.02072	0.00049	193	31	135	2	132	3
12.1	12479	5557	195	2.25	0.04791	0.00669	0.13448	0.01830	0.02036	0.00063	95	279	128	16	130	4
13.1	15590	7497	238	2.08	0.04916	0.00081	0.14027	0.00217	0.02070	0.00050	155	29	133	2	132	3
14.1	12519	3180	136	3.94	0.06189	0.00166	0.17726	0.00431	0.02077	0.00054	670	25	166	4	133	3
15.1	12134	4294	155	2.83	0.04984	0.00143	0.14216	0.00376	0.02069	0.00054	188	28	135	3	132	3
16.1	17451	7065	253	2.47	0.06115	0.00169	0.17862	0.00448	0.02119	0.00056	645	25	167	4	135	4
17.1	12582	6264	194	2.01	0.05266	0.00129	0.14976	0.00337	0.02063	0.00052	314	26	142	3	132	3
18.1	7866	4485	140	1.75	0.06137	0.00701	0.17322	0.01910	0.02047	0.00061	652	256	162	17	131	4
19.1	6373	3397	116	1.88	0.07566	0.00315	0.21896	0.00806	0.02099	0.00065	1086	33	201	7	134	4
20.1	18319	5773	227	3.17	0.06795	0.00161	0.19885	0.00428	0.02123	0.00055	867	24	184	4	135	3
21.1	12176	3979	144	3.06	0.05051	0.00136	0.14196	0.00352	0.02039	0.00053	219	27	135	3	130	3
22.1	12214	2929	126	4.17	0.05736	0.00149	0.16887	0.00401	0.02136	0.00056	505	26	158	3	136	4

Note: ***Radiogenic lead. Isotopic ratios and ages were corrected by common lead, following the methods reported by Andersen (2002)

.

Note 2: LA–ICPMS zircon U–Pb dating

Zircons were separated by heavy-liquid and magnetic methods. Cathodoluminescence images were used to check the internal structures of individual zircon grains and to select positions for analyses. Zircon U-Pb dating was performed using laser ablation microprobe–multicollector–inductively coupled plasma mass spectrometry (LA-ICPMS) at the Institute of Geology and Geophysics, Chinese Academy of Sciences, Beijing, China. The spot diameter for each analysis is 50 μm, and data were collected during 80 s of ablation after approximately 20 s of background counting. U-Th-Pb isotope ratios were measured relative to the standard material (NIST610) with a recommended $^{206}Pb/^{238}U$ age of 1065.4 ± 0.6 Ma (Wiedenbeck et al., 1995) and were calculated using the GLITTER 4.0 (GEMOC) software (Jackson et al., 2004). Common lead was corrected using the common lead correction function proposed by Anderson (2002). The plotting of concordia diagrams, age spectra, and age calculations were made using ISOPLOT (version 3.0) (Ludwig, 2003). The detailed analytical technique was described in Xie et al. (2008). Uncertainties on individual analyses are reported at the 1-sigma level; mean ages for pooled $^{206}Pb/^{238}U$ results are reported at the 2-sigma level.

References cited:

Anderson, T., 2002, Correction of common lead in U-Pb analyses that do not report ^{204}Pb: Chemical Geology, v. 192, p. 59-79.

Jackson, S.E., Pearson, N.J., Griffin, W.L., and Belousova, E.A., 2004, The application of laser ablation-inductively coupled plasma-mass spectrometry (LA-ICPMS) to in situ U–Pb zircon geochronology: Chemical Geology, v. 211, p. 47-69.

Ludwig, K.R., 2003, ISOPLOT 3.0: A Geochronological Toolkit for Microsoft Excel: Berkeley Geochronology Center Special Publication, v. 4, p. 71.

Wiedenbeck, M., Alle, P., Corfu, F., Griffin, W.L., Meier, M., Oberli, F., von Quadt, A., Roddick, J.C., and Spiegel, W., 1995, Three natural zircon standards for U-Th-Pb, Lu-Hf, trace element and REE analyses: Geostandards. Newsletter – Journal of Geostandar, v. 19, p. 1-23.

Xie, L.W., Zhang, Y.B., Zhang, H.H., Sun, J.F., and Wu, F.Y., 2008, In situ simultaneous determination of trace elements, U-Pb and Lu-Hf isotopes in zircon and baddeleyite: Chinese Science Bulletin, v. 53, p. 1565-1573.